UC San Diego

UC San Diego Previously Published Works

Title

Sizing of energy storage systems for connection power reduction and power smoothing of electric vehicle charging plazas

Permalink

https://escholarship.org/uc/item/8h96v6qq

Journal

International Journal of Electrical Power & Energy Systems, 172

ISSN

0142-0615

Authors

Lappalainen, Kari

Kleissl, Jan

Publication Date

2025-11-01

DOI

10.1016/j.ijepes.2025.111347

Copyright Information

This work is made available under the terms of a Creative Commons Attribution License, available at https://creativecommons.org/licenses/by/4.0/

Peer reviewed

eScholarship.org Powered by the California Digital Library
University of California

Sizing of energy storage systems for connection power reduction and power smoothing of electric vehicle charging plazas

Authors:
Kari Lappalainen[1], kari.lappalainen@tuni.fi, phone: +358505663117
Jan Kleissl[2], jkleissl@ucsd.edu
[1]Tampere University, Electrical Engineering Unit, FI-33101 Tampere, Finland
[2]University of California, San Diego, Center for Energy Research and Department of Mechanical and Aerospace Engineering, CA 92093-0411, United States

Abstract

The increasing number and charging power of electric vehicles might cause severe troubles for electrical grids motivating a need for investments in grid upgrades. The issues caused by high and intermittent energy demand of electric vehicle charging plazas can be solved with energy storage systems. This article covers sizing of stationary energy storage systems for electric vehicle charging plazas. Energy storage systems are sized to constrain the highest amount of power that the charging plaza takes from the grid below a particular power limit and restrict the rate of change in the grid power draw below a particular ramp rate limit. This is the first study concerning sizing of energy storage systems to smooth variations in the power that the charging plazas take from the grid. The power limit was altered from 10% to 100% and the ramp rate limit from 1 to 25 %/min in relation to the rated charging power of the charging plaza. This study was based on two years of measurement data compiled from eight direct current fast charging stations located in southern California, USA. The results show that the power and energy capacity requirements for an energy storage system used solely for reducing grid connection power below 50% increase only a little if the same energy storage system is used simultaneously also for reducing the rate of change in the grid power draw to comply with a ramp rate limit of 5 %/min or higher. However, use of the energy storage system for both purposes simultaneously increased the share of total electric vehicle charging energy that ran through the energy storage system increasing the degradation of the energy storage system.

Keywords: Energy storage sizing; Electric vehicle charging; Power smoothing; Connection power reduction; Ramp Rate Limit

Nomenclature

Δt	time difference between adjacent time steps (s)
C_{deg}	degradation rate of the ESS (-)
E_{ESS}	energy stored in the ESS (Wh)
$E_{ESS, full}$	energy stored in the fully charged ESS (Wh)
i	time step index (-)
$k_{[...]}$	coefficients in the degradation model (-)

N_{max}	maximum number of charge–discharge cycles (-)
N_{obs}	observed number of charge–discharge cycles (-)
P_{ESS}	power fed to the ESS (W)
P_{EV}	EV charging power (W)
P_{grad}	power addition/reduction corresponding to a lowered power gradient (W)
P_{grid}	power taken from the grid (W)
$P_{grid, ini}$	initial power taken from the grid (W)
$P_{grid, smo}$	smoothed power taken from the grid (W)
P_{RRL}	power addition/reduction corresponding to the applied RRL (W)

Abbreviations

DCFC	direct current fast charger
DOD	depth of discharge
ESS	energy storage system
EV	electric vehicle
PL	power limit
RR	ramp rate
RRL	ramp rate limit
UCSD	University of California, San Diego

1. Introduction

Along with the ongoing energy transition, a shift toward electrification of traffic is proceeding rapidly. Indeed, electric vehicles (EV) are becoming cheaper and their number is increasing heavily [1]: over 17 million EVs were sold globally in 2024 which is around eight times more than just five years earlier. By the end of 2024, almost 58 million EVs were registered globally. In the meanwhile, also the number of EV chargers is increasing and especially fast chargers, with high power levels, are becoming more and more common. There were over 5 million public EV chargers, including around 2 million fast chargers, globally at the end of 2024. However, home charging is still the most common way of EV charging.

The increasing number and power level of EV charging stations can cause serious troubles for electrical grids. The significantly increasing power demand of the charging stations gives rise to a need for investments in grid upgrades. Additionally, the highly intermittent nature of EV charging profiles of the charging stations endangers grid stability and makes demand forecasting more difficult. Highly intermittent energy demand causes similar issues for the grids than highly variable power production such as wind and photovoltaic power production. Several national requirements are already in force to limit ramp rates (RR) in injected power of grid-connected power plants [2]. Similar limitations for RRs in power drawn from the grid by customers with high-power levels, such as EV charging plazas, are expected in the future.

Several issues caused by increasingly common EV charging can be solved with energy storage systems (ESS). ESSs can be utilized for levelling the load profile of an EV charging plaza which reduces its

required connection power and thus reduces the need for investments in grid upgrades. Moreover, the ESSs can be employed to level off fast variations in the grid power draw of the charging plazas and for improving their power outage resilience. Economic operation of EV charging plazas incorporating several direct current fast chargers (DCFC) and an ESS necessitates efficient energy management to meet multiple objectives and constraints, such as cost minimization, load balancing, RR control, and customer satisfaction. Several approaches to optimize charging resource allocation have been introduced recently. For example, a quantum reinforcement learning based approach was proposed in [3], a spatiotemporal EV charging optimization scheme was presented in [4] and a two-stage spatiotemporal charging scheduling method was proposed in [5]. A recent review of ESSs for facilitating extensive grid integration of EV charging was given in [6] concluding that scalable ESS technologies with higher energy density and longer lifespans are vital for the future of EV integration.

ESSs play a vital role in modern electrical grids. In addition to facilitating large-scale grid integration of EV chargers they are important for alleviating grid integration of variable renewable power generation and for efficient energy management of the grids. Sizing of ESSs for power smoothing of variable renewable power generation has been studied intensively during recent years: for example, for photovoltaic power plants in [7]; for wind power plants in [8]; and for hybrid photovoltaic–wind power plants in [9]. Coordinated operation of ESSs with photovoltaic and wind power plants, hydrokinetic turbines and diesel generators in an autonomous grid was studied in [10] from a technical, environmental and economic point of view. Optimal sizing and energy management of a hybrid grid-connected microgrid including renewable power production, ESSs, and EV charging stations was investigated in [11]. Indeed, balancing multiple energy sources and using storage to manage variability in electricity production and demand is an important and timely topic given the rapid growth of electrification and renewable energy production along with the ongoing energy transition.

Several research groups have studied sizing of ESSs for EV charging plazas over the past few years. However, most of these studies have focused on using ESSs for peak load reduction. Several factors were found to impact sizing of the ESSs for reducing peak loads: EV charging plaza size [12, 13]; temporal resolution of EV charging data [12]; and charging plaza capacity factor [14]. Optimal ESS sizing for EV charging peak load reduction was studied in [15, 16] considering also resilience to power outages. The results of [16] show that peak load reduction and power selling to the utility grid can be increased by increasing the ESS energy capacity without significantly affecting the optimal length of the resilience window. Another popular research area has been utilization of ESSs for reducing electricity costs of charging plazas. Sizing of ESSs was investigated in [17, 18] considering costs of electricity and the ESS. It was found in [18] that reduction in annual electricity costs might be several times higher than the annual cost of the ESS. Optimal sizing of ESSs for maximizing profits of EV charging plazas having photovoltaic power production was examined in [19]. Reduction of EV user waiting times by ESSs was examined in [20]. In addition to light-duty vehicles, also heavy-duty vehicles are becoming electrified with an increasing pace [1]. Sizing of ESSs for cost minimization of heavy-duty EV charging was studied in [21]. Despite all the research effort related to use of stationary ESSs to support EV charging, use of ESSs to restrict variations in the grid power draw of the charging plazas has not been studied to date. This study overcomes this knowledge gap.

Most of the former research on sizing of ESSs for EV charging plazas utilized synthetic EV charging demand profiles in place of using actual measurement data from EV charging stations. Creation of synthetic charging profiles requires various assumptions and simplifications: for example, probabilities of EV driving behavior were utilized in [15, 16, 18]; measurement-based probability distributions of EV arrival times in [13, 20]; data of fuelling stations popular times in [21]; and daily commuting profiles of EVs in [17]. Simulations based on actual measurement data were performed in [12, 14, 19]. Synthetic charging demand profiles were compared with actual measurements in [22]. Use of synthetic charging profiles in place of measurements increases uncertainty of the obtained results. To avoid that uncertainty, charging profiles generated based on actual charging session measurement data were used in this study. It was found in [23] that no statistically noteworthy difference exist between generation of charging profiles based on measurements from charging stations (power factor, current, and voltage of chargers) or charging session measurements (energy dispensed and beginning and ending time of the charging). Moreover, temporal resolution of charging demand profiles affect the obtained results. The results of [24] show that temporal resolution has a strong effect on the highest charging powers of EV fleets: the peak powers for a 1 min resolution were considerably higher than those for a 1 h resolution. Moreover, the difference was found to increase with increasing power level of the charging stations. It was found in [12] that 2 min is a sufficient averaging time interval for sizing ESSs for EV charging peak load reduction while use of 1 h intervals leads to considerably distorted results. In this study, temporal resolution of 1 s was used when generating charging profiles, while in most earlier studies the resolution used has varied from 10 s [25] to 2 h [26].

In this article, sizing of stationary ESSs to perform concurrent connection power reduction and power smoothing of electric vehicle charging plazas is studied. The ESS was used to restrict the highest amount of power taken from the grid below a particular power limit (PL) and simultaneously to restrict the rate of change in the grid power draw to comply with a particular ramp rate limit (RRL). The PL and RRL were expressed in relation to the rated charging power of the charging plaza. The PL was altered from 10% to 100% and the RRL from 1 to 25 %/min to study their effects on ESS sizing. The study is based on two years of measurement data compiled from eight DCFC stations. In total over 18 thousand measured charging sessions were analyzed. The main novelty of this study is that this is the first time that sizing of ESSs to smooth variations in the power that the charging plazas take from the grid is studied. Moreover, a novel rule-based ESS control strategy for smoothing variations in the power that the charging plazas take from the grid is proposed. The rest of the article is organized as follows. The measurement data and the ESS control strategy used are introduced in Section 2. Section 3 presents the results of the study, and they are further discussed in Section 4. Finally, Section 5 gives the conclusions.

2. Data and methods

2.1. Electric vehicle charging data

Two years of EV charging data from eight ChargePoint DCFC stations situated on the campus of the University of California, San Diego (UCSD) was utilized. In total 18,354 charging sessions took place at the eight DCFC stations during the period from September 2022 to August 2024. Each charging session

measured includes the name of the charging station, the energy dispensed, and the times when charging started and ended. The DCFC stations were not able to schedule charging or charge flexibly. Thus, the charging typically occurred at the maximum charging power of the EV or the rated power of the station whichever was less. Charging sessions without recorded energy or duration for the charging were excluded leading to 18,219 charging sessions that were analyzed. Each DCFC station has a rated power of 62.5 kW, and each of them is paired with another one so that if only one of them is occupied, then the maximum power supply to a single EV doubles to 125 kW. Sessions with power higher than the rated power of a single station were modeled as if there was only 62.5 kW available by cutting out the excess energy. A time series of charging power was created for each DCFC station with a sampling rate of 1 s by assuming charging power to be constant for each EV charging session. Generated time series of power were combined to create a virtual EV charging plaza with eight DCFC stations and a total rated charging power of 500 kW.

Table I presents the capacity factor, total energy dispensed, total charging duration and number of the charging sessions for the eight DCFC stations. The number of charging sessions ranged from around 1,200 to 3,900. The Osler DCFC stations were the most utilized in terms of the number and total duration of charging sessions as well as the energy dispensed. Their capacity factors were around 15% while the capacity factors of the other stations ranged from 4.8% to 10.1%. The time distribution of the average EV charging power for the eight DCFC stations is presented in Fig. 1. Each DCFC station has similar trend; the most common time for charging EVs was from 9 a.m. to 9 p.m. while charging was rarer at nights.

Table 1

Capacity factor, total energy dispensed, total charging duration, and number of charging sessions for the eight DCFC stations during the measurement period of two-years.

Station	Capacity factor (%)	Energy dispensed (MWh)	Total duration (h)	Charging sessions
ATHENA DCFC 2	6.81	42.3	1,192	1,626
ATHENA DCFC 3	4.89	27.2	855	1,182
ATHENA DCFC 4	4.75	31.8	832	1,180
ATHENA DCFC 5	6.77	46.8	1,185	1,762
ATHENA DCFC 6	10.10	65.1	1,767	2,455
NUEVO WEST DCFC 2	9.44	54.5	1,652	2,210
Osler DCFC 1	15.07	105.9	2,637	3,891
Osler DCFC 2	15.01	113.9	2,625	3,913

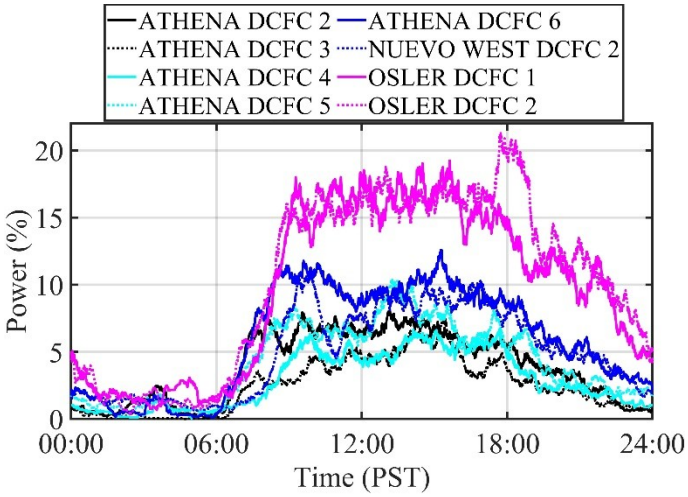


Fig. 1. Daily average EV charging power for the eight DCFC stations during the two-year period. The powers are in relation to the rated charging power of a DCFC station (62.5 kW).

Some trends in EV charging were observed. The monthly energy dispensed and number of hours of charging had an increasing trend. The average model year of the EVs that charged at the DCFC stations increased 1.6 years or so during the period of two-years. The average age of the EVs, calculated using the average model year, was around 4 years. No noteworthy changes in EV models took place during the period with the Nissan Leaf being the most common one.

2.2. Energy storage system control strategy

The ESS was controlled by a rule-based control strategy to restrict the highest amount and rate of change of the grid power draw P_{grid} of the charging plaza to comply with the applied PL and RRL, respectively. The PL was varied from 5% to 100% and the RRL from 1 to 25 %/min of the rated charging power of 500 kW. The power limiting control of the ESS works as follows. The ESS is discharged when the EV charging power P_{EV} of the charging plaza is more than the PL and charged when P_{EV} is less than the PL until the ESS is fully charged, i.e. when the energy stored in the ESS E_{ESS} equals the energy stored in the fully charged ESS $E_{ESS,\,full}$. The power limiting control strategy, introduced in [12], is illustrated in Fig. 2.

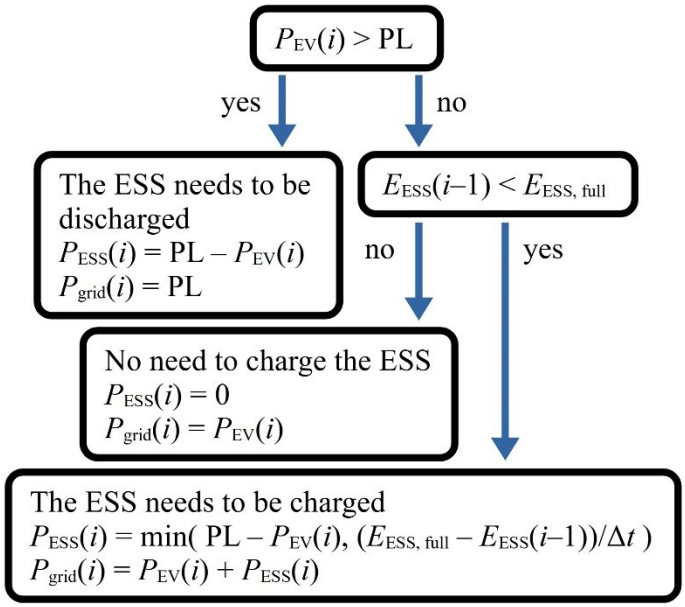


Fig. 2. Flowchart of the ESS control strategy for power limiting.

The power smoothing control of the ESS smooths each shift in the charging power of the charging plaza so that the grid power draw complies with the applied RRL. When an EV starts charging, the charging power of the charging plaza increases faster than the RRL and a part of the energy is taken from the ESS. Correspondingly, the ESS is charged after the EV charging session ends to lower the grid power draw with the applied RRL. To make sure that the average energy level of the ESS does not drift gradually, the gradient for each ramp (power addition/reduction P_{grad}) to a new power value was calculated so that the energy shortfall of the ESS after the ramp equals the energy charged to the ESS if the new power level was lowered to zero with the applied RRL (power addition/reduction P_{RRL}). This also guarantees that the applied RRL is always respected. Fig. 3 illustrates the ESS control strategy for power smoothing. $P_{grid, ini}$ is the initial power taken from the grid that needs to be smoothed and $P_{grid, smo}$ is the smoothed grid power. If only power smoothing is applied EV charging power P_{EV} acts as $P_{grid, ini}$. If both power limiting and smoothing are applied, $P_{grid, ini}$ is P_{grid} given by the power limiting control of the ESS. Positive power of the ESS P_{ESS} indicates charging and negative P_{ESS} indicates discharging of the ESS. The ESS was full of charge in the beginning of the two-year period. Losses and degradation of the ESS and losses in cables were not considered. This simple methodology was selected as it is well suited to determining technology independent ESS requirements for EV charging plazas.

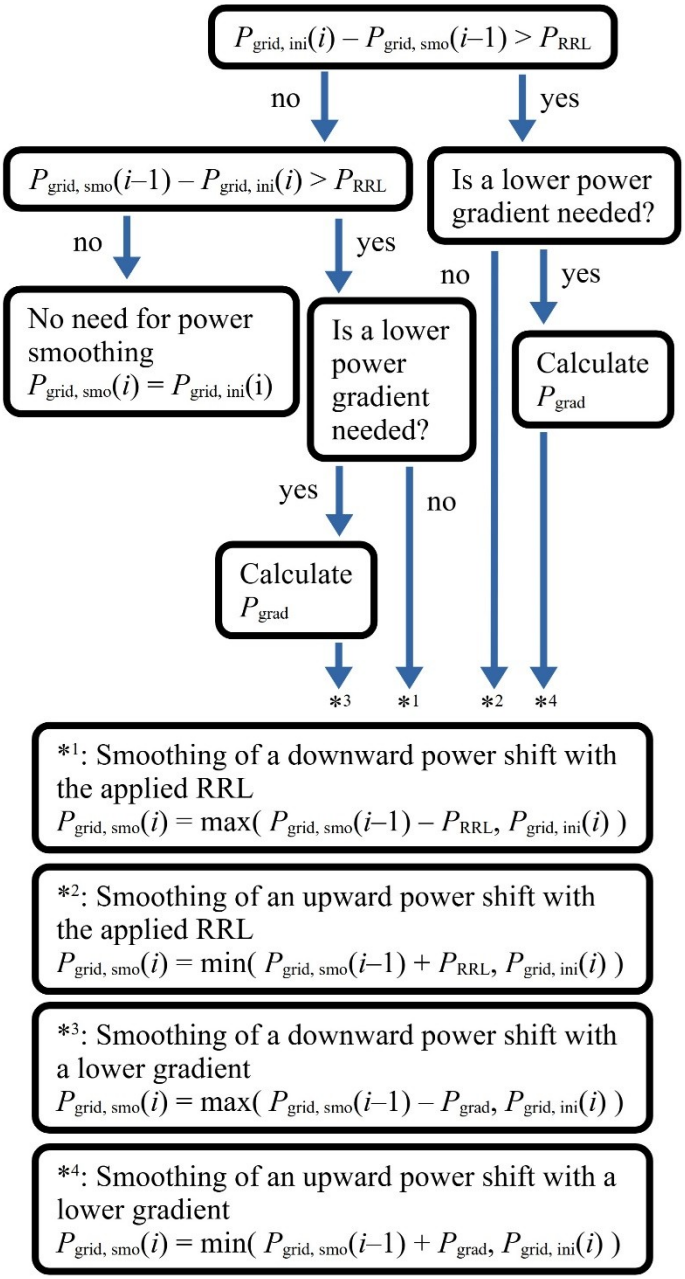


Fig. 3. Flowchart of the ESS control strategy for power smoothing. P_{RRL} and P_{grad} are the power additions/reductions corresponding to the applied RRL and a lowered power gradient, respectively. A time step index is denoted by i and Δt is the time difference between adjacent time steps.

Fig. 4 illustrates the ESS control strategy. Fig. 4 (a) shows operation of the ESS when it is used solely for connection power reduction, i.e., without power smoothing. The EV charging power P_{EV} rises above the applied PL of 5% two times at 450 s and 1150 s. The part of P_{EV} that exceeds the PL is taken from the ESS and the ESS is charged when P_{EV} drops below the PL until the ESS is fully charged. Fig. 4 (b) illustrates the operation of the ESS when it is used solely for power smoothing, i.e., without connection power reduction. Each change in P_{EV} is smoothed to make the grid power draw compliant with the applied RRL. The RR by which the power taken from the grid is altered equals the applied RRL except at the power fall starting at 600 s and at the power rise starting at 1150 s. In the case of the power rise at 1150 s, the rise of EV charging power starts from a non-zero level as there is already one EV charging when another EV

starts to charge. The RR by which the power taken from the grid is raised is lower than the applied RR so that the energy shortfall of the ESS after that change equals the energy charged to the ESS when the power taken from the grid was lowered to zero with the applied RRL after the change in the EV charging power at 1450 s. Fig. 4 (c) shows operation of the ESS when it is used for both connection power reduction and power smoothing. In that case, the grid power draw is limited during the two highest peaks of P_{EV}, which exceed the applied PL of 5%, and smoothed so that it complies with the applied RRL.

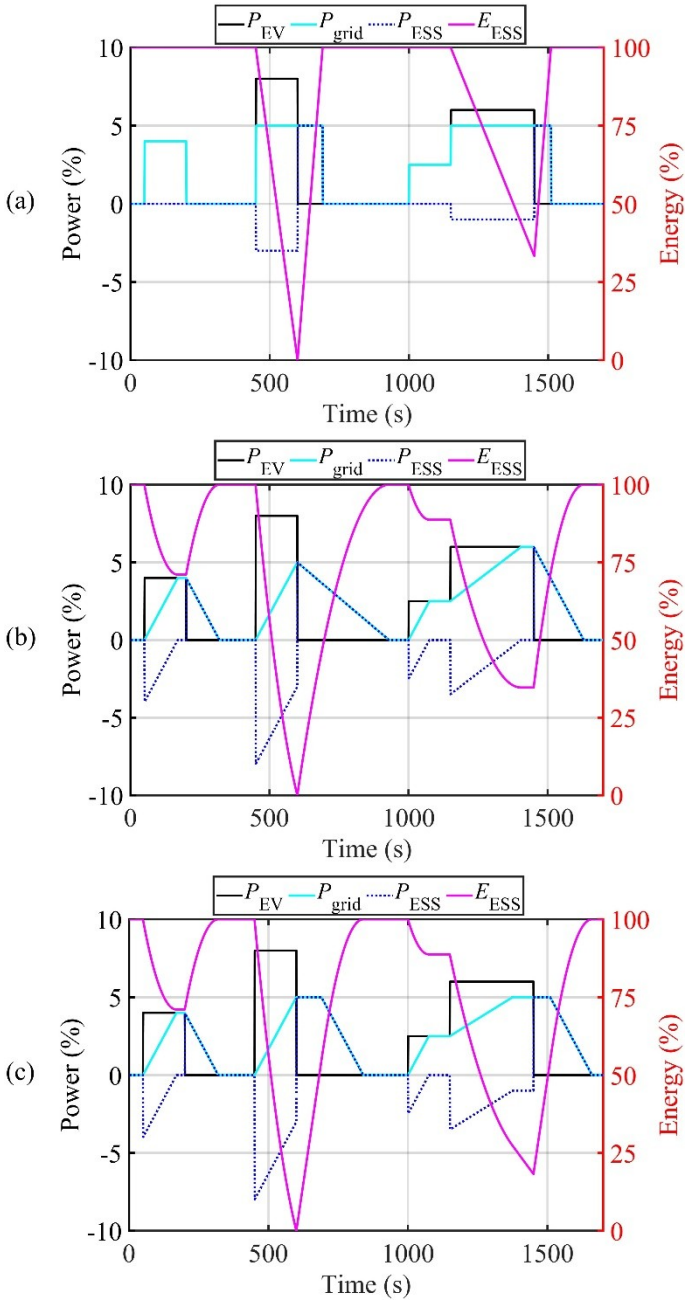


Fig. 4. Example of EV charging power P_{EV}, power taken from the grid P_{grid}, power of the ESS P_{ESS}, and energy of the ESS E_{ESS} for 8 DCFC stations with power limit of 5% (a), ramp rate limit of 2 %/min (b) and both power limit of 5% and ramp rate limit of 2 %/min. The powers are in relation to the rated EV charging power.

2.3. Energy storage system degradation

Cycling induced degradation of the ESSs was estimated based on the numbers and amplitudes of charge–discharge cycles. For that analysis, the ESS was selected to be a Li-ion battery ESS. The amplitude of the cycles was expressed as depth of discharge (DOD) which denotes how large share of the total energy capacity of the ESS is used for a charge–discharge cycle. The charge–discharge cycles and their DODs were calculated using the Rainflow cycle counting algorithm [27] that is commonly used for fatigue analysis due to its capability to identify and calculate sub-cycles inside larger cycles [28]. Each charge–discharge cycle degrades a battery ESS and there is a certain number of cycles for each DOD that the ESS is expected to withstand without too high energy capacity loss. Typically, this maximum number of cycles $N_{\max}$ is defined for a capacity loss of 20% [29]. Cycling induced degradation caused by charge–discharge cycles observed for a certain DOD can be calculated by dividing the number of these cycles N_{obs} by $N_{\max}$ of that DOD value. The total cycling induced degradation rate C_{deg} of the ESS can be calculated as the sum of cycling induced degradation caused by all DODs, i.e., as

$$C_{deg} = \sum_{DOD=0\%}^{100\%} \frac{N_{obs}(DOD)}{N_{max}(DOD)}. \quad (1)$$

There are several methods for calculating $N_{\max}$ for different battery technologies [30]. For this study, a simple power model was selected where $N_{\max}$ for each DOD value is expressed as

$$N_{max}(DOD) = k_1 DOD^{-k_2}, \quad (2)$$

where k_1 and k_2 are model coefficients [30]. Values k_1 = 4000 and k_2 = 1.632, used in [29], were selected. These values are suitable for a high-quality $LiFePO_4$ cells [31]. The maximum number of cycles that the ESS is expected to withstand calculated using Eq. (2) and these values is presented in Fig. 5 as a function of the DOD.

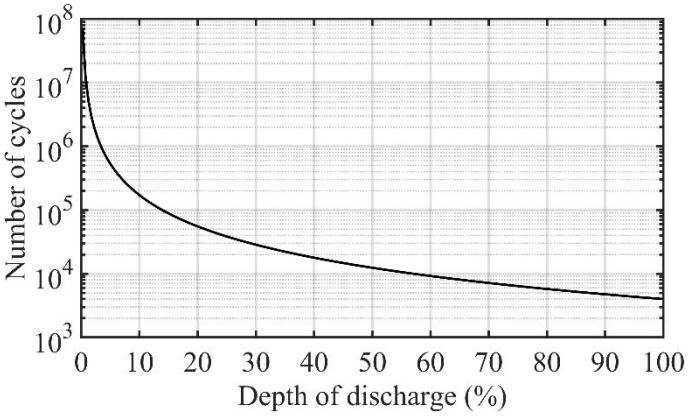


Fig. 5. Number of charge–discharge cycles that the ESS is expected to withstand with at most 20% energy capacity loss as a function of the DOD of the cycles.

3. Results

3.1. Required capacity of the energy storage system

Fig. 6 presents the highest ESS charging and discharging powers, the highest EV charging power, and the highest grid power draw observed during the two-year period for the charging plaza of 8 DCFC

stations as a function of the PL. In Fig. 6 (a), the ESS was used solely for power limiting, i.e., no RRL was applied. In that case, the highest power taken from the grid was equal to the PL for PLs lower than the highest EV charging power. In this PL region, the highest ESS discharging power decreased linearly with increasing PL as the sum of the grid power draw and the ESS discharging power equals the EV charging power. At low PLs, the highest ESS charging power was equal to the highest power taken from the grid and the PL, and at PLs higher than the highest EV charging power it was zero as there was no longer a need to limit the grid power draw. Between these two regions, there is a region where the highest ESS charging power fluctuates. The reason for this is that, in this region, when the highest ESS charging power occurs, the power taken from the grid is not totally used for charging the ESS but part of it is used for EV charging. Thus, the highest ESS charging power depends on the smallest EV charging power during ESS charging. This behavior, which is a result of the rule-based ESS control strategy used, was explained in more detail in [12].

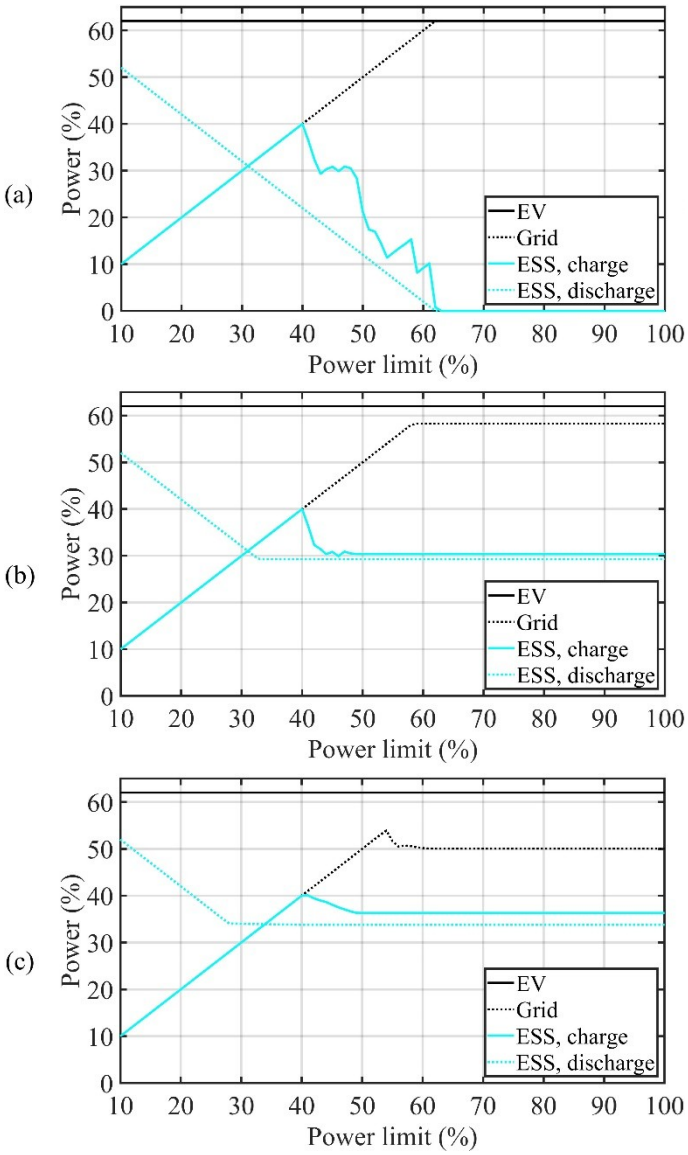


Fig. 6. The highest EV charging power, highest power taken from the grid, and highest ESS charging and discharging powers during the two-year period for the 8 DCFC stations without power smoothing (a) and with ramp rate limits of 20 %/min (b) and 2 %/min (c) as a function of the power limit. The powers are in relation to the rated charging power.

Use of the ESS for power smoothing in addition to limiting the grid power draw affects the highest power taken from the grid and the highest ESS charging and discharging powers observed during the two-year period. This is illustrated in Figs. 4 (b) and (c) where ramp rate limits of 20 and 2 %/min were applied, respectively. Application of RRLs increased the highest ESS charging and discharging powers at high PLs: the highest ESS charging and discharging powers were not zero after the PL had reached the highest EV charging power, and there was no longer a need to limit the power drawn from the grid, as the ESS was still used for power smoothing. The levels to which the highest ESS charging and discharging powers settled were the higher the stricter was the RRL. This is expected as a stricter RRL means higher need for power smoothing and thus higher ESS powers are needed. At high PLs, the highest ESS charging powers were higher than the highest ESS discharging powers. When an RRL is applied it restricts the growth rate in power taken from the grid and the highest power taken from the grid does not reach the highest EV charging power anymore. Thus, at high PLs, the highest power drawn from the grid decreased with increasing RRL. The highest EV charging power was constant at 62% in all cases, as the EV charging timeseries were not controlled at all.

Fig. 7 presents the required ESS power capacity for various RRLs as a function of the PL. The required ESS power capacity means the highest ESS charging or discharging power that was needed to fulfill the tasks of the ESS during the two-year period. At low PLs, the highest discharging power determines the required ESS power capacity, while at high PLs the highest charging power is the determining factor as can be seen in Fig. 6. When no RRL was applied, the ESS power requirement decreased first as the PL increased due to the linearly decreasing highest ESS discharging power. After that it increased due to the linearly increasing highest ESS charging power. That increase was followed by a region characterized by fluctuations of the highest ESS charging power after which the power requirement was zero at PLs higher than 62% or so. A similar behavior of the ESS power requirement was reported in [12]. Application of an RRL alters the curve greatly, especially at high PLs where even the loosest RRL (20 %/min) yields much higher power requirements. The ESS power capacity requirement increased with decreasing RRL and its variation with varying PL became smoother. With the strictest RRL studied (1 %/min), the ESS power requirement was quite constant at PLs higher than 21% or so. The results of Fig. 7 mean that, if an ESS is used to limit grid connection power below 50% in relation to the rated charging power, use of the same ESS also for smoothing the grid power draw with an RRL from 5 to 20 %/min has only minor effect on the required power capacity of the ESS. With an RRL of 1 %/min, which was the strictest RRL studied, the effect is larger depending on the applied PL.

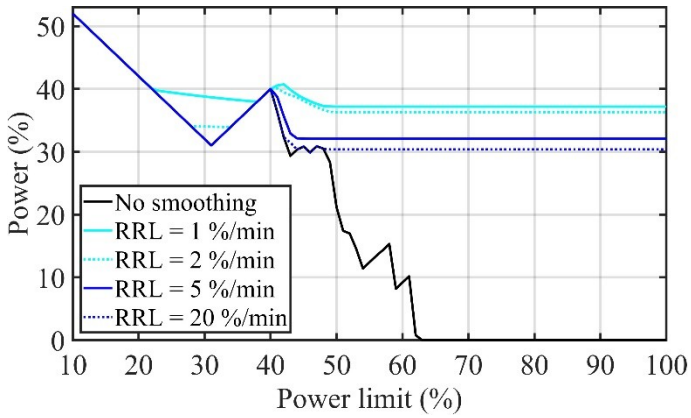


Fig. 7. Required power capacity of the ESS in relation to the rated charging power during the two-year period for various ramp rate limits as a function of the power limit.

The required power capacity of the ESS is presented in Fig. 8 as a function of the applied PL and RRL. At low PLs, the required ESS power decreased strongly with increasing PL and was independent of the RRL which can also be seen in Fig. 7. At higher PLs, the required power capacity of the ESS decreased, in general, with increasing RRL. However, some variations existed that are clearly visible at an RRL range from 9 to 15 %/min.

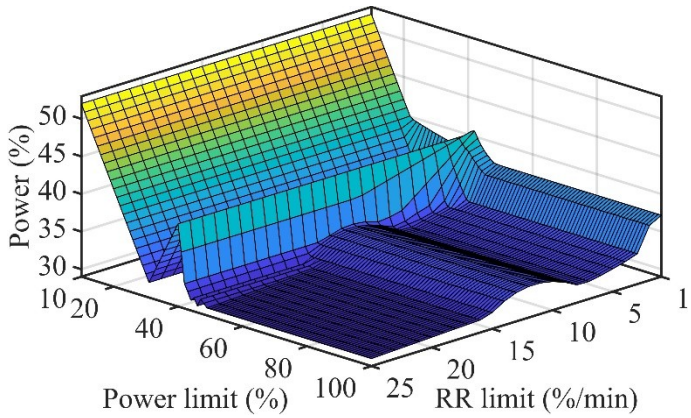


Fig. 8. Required power capacity of the ESS in relation to the rated charging power during the two-year period as a function of the power limit and ramp rate limit.

The required ESS power capacity for various RRLs is shown in Fig. 9 as a function of the PL. The required power capacity decreased with increasing PL as the need for levelling EV charging power demand decreased. When the ESS was used solely for connection power reduction, the ESS did not need to operate at PLs higher than 62% or so, meaning that the required energy capacity also goes to zero at this point, consistent with the required power capacity in Fig. 7. This finding is in line with [12] where ESSs were used solely for reducing grid connection power. The ESS energy requirement increased with decreasing RRL as the need for power smoothing increased. This effect was the stronger the higher was the PL and only minor differences existed between different RRLs at PLs lower than 20% or so. These results mean that use of an ESS to smoothing the grid power draw in addition to limiting its maximum values has only minor effect on the required energy capacity of the ESS with the exception of the strictest RRLs studied.

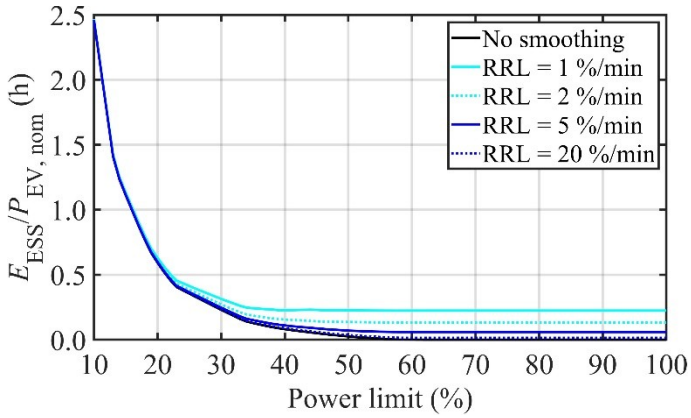


Fig. 9. Required energy capacity of the ESS in relation to the rated charging power during the two-year period for various ramp rate limits as a function of the power limit.

Fig. 10 shows the required ESS energy capacity as a function of the applied PL and RRL. The required energy capacity decreased strongly with increasing PL and RRL at low values of the limits. On the other hand, there is a large area, roughly when the PL was higher than 35% and the RRL higher than 5 %/min, where the energy capacity was relatively constant having values lower than 0.15 h.

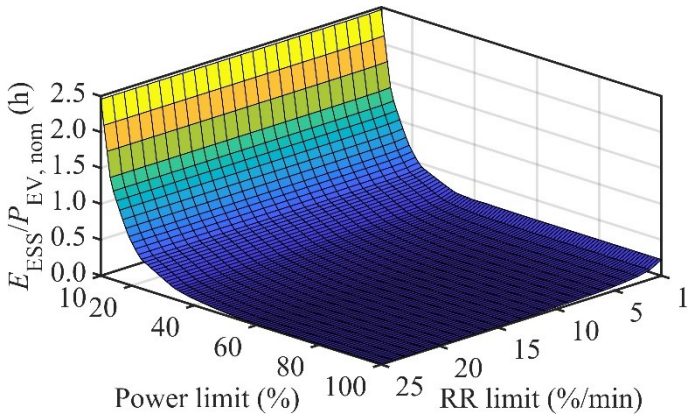


Fig. 10. Required energy capacity of the ESS in relation to the rated charging power during the two-year period as a function of the power limit and ramp rate limit.

3.2. Utilization and degradation of the energy storage system

In addition to the actual sizing parameters also strain of the ESSs for limiting the grid power draw of the charging plaza and its rate of change was considered. The energy that ran through the ESS was used as an indicator of the ESS strain as a proxy for degradation. Moreover, cycling induced degradation rates were examined. The required energy capacity of the ESS for each combination of the PL and RRL presented in Fig. 10 was used as the energy capacity of the ESS to calculate the DODs needed to obtain the degradation rates. Fig. 11 presents the share of total EV charging energy that ran through the ESS for various RRLs as a function of the PL. First, the share of energy that ran through the ESS decreased with increasing PL after which it leveled off. If the ESS was used solely for connection power reduction, only a minor share of energy ran through the ESS at PLs higher than 40% or so and finally the share of energy went to zero for PLs higher than 62% or so when the PL reached the highest EV charging power. These results are in agreement with [12]. The share of energy that ran through the ESS increased with decreasing RRL as the

need for power smoothing increased. This effect was much stronger for the share of energy that ran through the ESS than it was for the required ESS capacity (Figs. 9 and 10). The constant level of the share of energy at PLs higher than the highest EV charging power was 17.1% for a strict RRL of 1 %/min while it was only 5.2% for an RRL of 5 %/min.

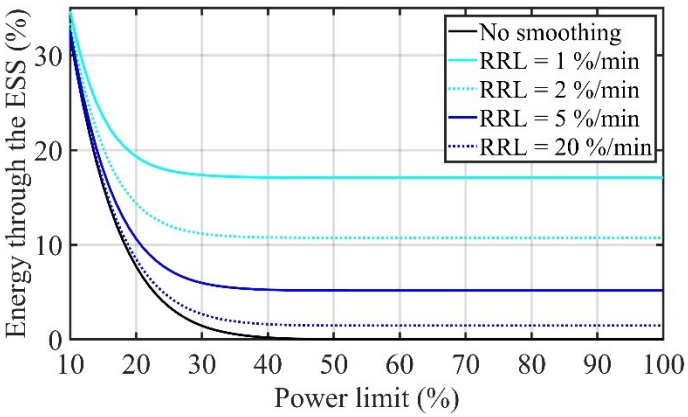


Fig. 11. Share of total EV charging energy that ran through the ESS during the two-year period for various ramp rate limits as a function of the power limit.

The share of total EV charging energy that ran through the ESS is shown in Fig. 12 as a function of the applied PL and RRL. At low values of these limits, the share of energy decreased heavily when the limits increased. This decrease slowed down with increasing values of the limits. The share of energy that ran through the ESS was independent of the PL at PL values higher than 62% or so. The share of energy was less than 5% if the PL was at least 29% and the RRL no less than 7 %/min.

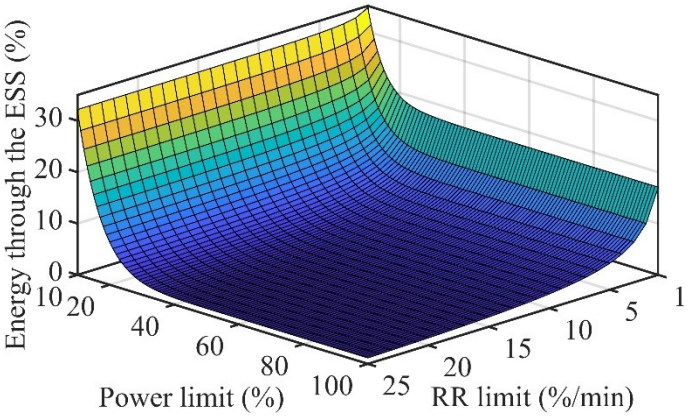


Fig. 12. Share of total EV charging energy that ran through the ESS during the two-year period as a function of the power limit and ramp rate limit.

Fig. 13 presents the observed number of charge–discharge cycles for various ramp rate limits with a power limit of 25% as a function of the depth of discharge. The number of cycles decreased heavily with increasing DOD and there were only few cycles with a DOD of over 60%. This means that only a small portion of the ESS energy capacity was utilized during typical charge–discharge cycles. The number of cycles was, in general, the lowest when the ESS was used solely for connection power reduction and increased with decreasing RRL which is reasonable as the need for power smoothing increased. However,

the differences were small with DODs higher than 50% or so. These results are in line with the results of Figs. 11 and 12 denoting that the usage of the ESS increased with decreasing RRL.

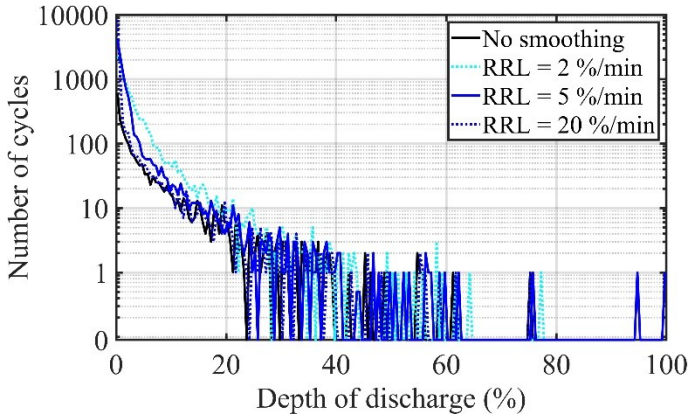


Fig. 13. Observed number of charge–discharge cycles of the ESS during the two-year period for various ramp rate limits with a power limit of 25% as a function of the depth of discharge.

The degradation rate of the ESS for various RRLs is presented in Fig. 14 as a function of the applied PL. In general, the degradation rate increased with increasing PL. If the ESS was used solely for power limiting the degradation rate was zero for PLs higher than the highest EV charging power. The reason for this is that in that case there is no need to use the ESS, i.e., there are no charge–discharge cycles causing cycling induced degradation of the ESS. The degradation rate increased with decreasing RRL at RRLs lower than 50% or so and increased with increasing RRL at higher RRLs.

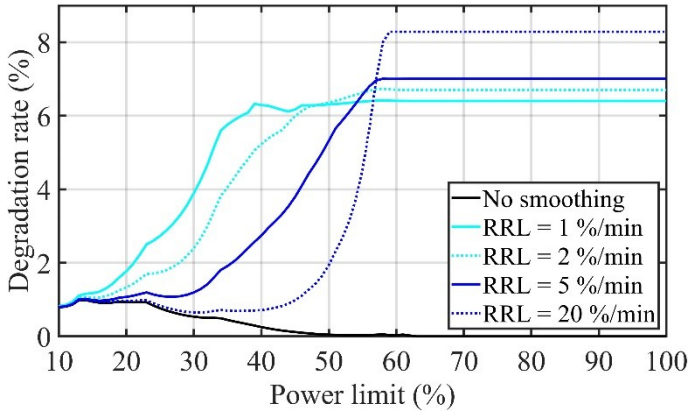


Fig. 14. Degradation rate of the ESS during the two-year period for various ramp rate limits as a function of the power limit.

The degradation rate of the ESS is presented in Fig. 15 as a function of the applied PL and RRL. In general, the degradation rate increased with increasing PL. The behavior of the degradation rate as a function of the RRL depends on the applied RRL as demonstrated in Fig. 14. The degradation rate increased with decreasing RRL at low RRLs and increased with increasing RRL at high RRLs. The degradation rate was less than 9% during the two-year period for all combinations of the PL and RRL. The highest degradation rates were obtained for combinations of high PL and high RRL. The required energy capacity in Fig. 10 decreased with increasing PL and RRL and only a low energy capacity was needed for power limiting and smoothing for combinations of high PL and high RRL. An ESS with a low energy

capacity is more prone to degradation than an ESS with a higher capacity since a lower energy capacity means that a charge–discharge cycle with a certain absolute magnitude yields a higher DOD and thus leads to stronger degradation of the ESS.

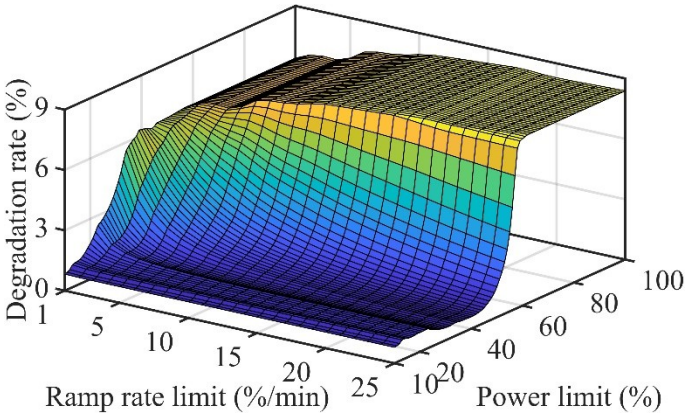


Fig. 15. Degradation rate of the ESS during the two-year period as a function of the ramp rate limit and power limit.

The results of this study show that the power and energy capacity requirements for an ESS used solely for reducing grid connection power below 50% increase only a little if the same ESS is used simultaneously also for reducing the rate of change in the grid power draw. However, use of extremely strict RRL for the grid power draw has a higher effect on the ESS power and energy requirements. Moreover, it was shown that use of the ESS for these two purposes simultaneously increases the share of total EV charging energy that ran through the ESS compared to use of the ESS solely for reducing connection power. However, the results show that use of the ESS also for power smoothing has only a weak effect on the cycling induced degradation of the ESS at PLs lower than 20% or so. At higher PL, use of the ESS for the two purposes resulted in stronger degradation and thus shorter lifetime of the ESS. The results regarding a scenario in which the ESS is used solely for reducing connection power are in line with the earlier results presented in [12]. As this is the first study of sizing ESSs for power smoothing of EV charging plazas, there is no reference to which the results achieved in the case of using the ESS for both limiting the grid power draw of the charging plaza and also limiting its rate of change could be compared. A comparison of the proposed ESS control strategy for smoothing variations in the power that the charging plazas take from the grid with other control strategies developed for that purpose would have been an interesting and useful addition to this article. However, earlier methods do not exist forbidding such a comparison.

4. Discussion

The simulation methodology used in this study contains some simplifications. EV charging power demand profiles were generated based upon EV charging session measurements by assuming constant power rate for each EV charging session between the times when charging started and ended. However, in reality the EV charging power is typically not constant for the whole charging time but decreases progressively at state of charge over 80% or so. Differences between actual electrical measurements and time series of charging power created by this simple approach were studied in [23], and they were found to

be typically small. In addition to usually small differences in power time series, both approaches yield the same amount of dispensed energy for each charging session. Moreover, losses and real-time degradation of the ESS were not considered. Thus, capacity requirements for actual ESSs are supposed to be somewhat higher than those presented in this article. Furthermore, the ESS control strategy used did not consider electricity prices and thus was not economically optimal. A control strategy that optimizes the ESS usage economically based on time-of-use electricity prices might affect the required ESS capacity. Moreover, there are various requirements and regulatory constraints related to practical implementation of the control strategy that also affect optimal size of the ESS. Such considerations including economic and practical implementation points of view are useful topics for future work.

The selected ranges of the PL and RRL need to be considered when analyzing the results. Use of too narrow ranges might be misleading. The range for PL was selected to be wide, from 10% to 100% of the rated charging power of the charging plaza. The lower limit of 10% was selected since the required connection power for the charging plaza would be 5.6% if the demand profile was levelled off perfectly meaning that PLs lower than that are not feasible. On the other hand, 100% PL means that the grid connection power equals the total rated charging power of the charging plaza and PLs higher than that are not feasible either. Our reasoning behind the selection of the RRL range was the following. If limits will be placed for RRs in power drawn from the grid by customers with high-power levels, such as EV charging plazas, the limits would most likely be on similar range than the limits applied for RRs in injected power of grid-connected power plants. The RRLs for power plants that are already in force in different regions mostly range from 1 to 20 %/min, the most common value being 10 %/min [2, 32]. Thus, the RRL range for this study was selected to be from 1 to 25 %/min.

The measurement period also affects the results. A period of two years was selected to ensure representative results. The amounts of EVs and their charging stations as well as the levels of EV charging powers will continue increasing in the future. Increasing charging powers and utilization results will affect the ESS sizing. Effects of the charging plaza utilization rate and size on sizing of ESSs for reducing peak loads of EV charging plazas were studied in [14]. A corresponding study for sizing of ESSs for power smoothing of EV charging plazas is another future research topic to be considered. In future, EV charging plazas will be more often integrated with on-site renewable generation. That could yield substantial synergies for the ESS. Sizing of ESSs for EV charging plazas having on-site generation and development of efficient ESS control strategies for that purpose provide interesting topics for future work.

5. Conclusions

In this article, sizing of stationary ESSs for EV charging plazas to limit connection power and smooth the grid power draw was studied. The ESS limited the highest grid power draw below a PL and, at the same time, limited its rate of change below an RRL. The effects of these limits on sizing of the ESS were studied. The PL was altered from 10% to 100% and the RRL from 1 to 25 %/min in relation to the rated charging power of the charging plaza (500 kW). The study was based on over 18 thousand EV charging sessions measured from eight DCFC stations located in southern California, USA during a period of two years.

In general, the required size of the ESS, i.e., its energy and power capacities, decreased as the PL and RRL increased. Moreover, the share of total EV charging energy that ran through the ESS, i.e., the utilization rate of the ESS, decreased with increasing PL and RRL, respectively, as the need for limiting and smoothing EV charging power demand decreased. Based on the results, a relatively small ESS capacity is enough to decrease the required grid connection power of an EV charging plaza considerably while keeping the maximum rate of change in the power drawn from the grid fairly small. However, an ESS with high power and energy capacity is needed to make the grid power draw almost constant.

The results of this study show that the power and energy capacity requirements for an ESS used solely for reducing grid connection power increase if the same ESS is used simultaneously also for reducing the rate of change in grid power draw. The difference between these two scenarios was much higher in ESS power requirements than in ESS energy requirements, especially at high PLs. However, the difference in the ESS power and energy capacity requirements was small when the PL was less than 50% and the RRL at least 5 %/min in relation to the rated EV charging power. The difference in ESS power and energy requirements was clearly higher for stricter RRLs. However, use of the ESS for these two purposes simultaneously increased the share of total EV charging energy that ran through the ESS and the cycling induced degradation of the ESS. The share of energy that ran through the ESS was the higher the lower was the RRL.

Acknowledgments

K. Lappalainen was funded by the Research Council of Finland (funding decision 348701) and J. Kleissl by TotalEnergies.

Author contributions: CRediT

Kari Lappalainen: Conceptualization, Formal analysis, Methodology, Writing - Original Draft
Jan Kleissl: Conceptualization, Writing - Review & Editing

References

[1] International Energy Agency. Global EV Outlook 2025, https://www.iea.org/reports/global-ev-outlook-2025; 2025 [accessed 25 May 2025].

[2] Craciun B-I, Kerekes T, Sera D, Teodorescu R, Annakkage UD. Power Ramp Limitation Capabilities of Large PV Power Plants With Active Power Reserves. IEEE Transactions on Sustainable Energy 2017;8:573–581. https://doi.org/10.1109/TSTE.2016.2612121.

[3] Xu H, Zhang A, Wang Q, Hu Y, Fang F, Cheng L. Quantum Reinforcement Learning for real-time optimization in Electric Vehicle charging systems. Applied Energy 2025;383:125279. https://doi.org/10.1016/j.apenergy.2025.125279.

[4] Xiao T, Peng Y, Chen C. A temporal and spatial electric vehicle charging optimization scheme with DSO-EVA coordination framework. International Journal of Electrical Power and Energy Systems 2024;156;109761. https://doi.org/10.1016/j.ijepes.2023.109761.
[5] Wu H, Lan X, He Y, Wu AY, Ding M. Orderly charging of electric vehicles: A two-stage spatial-temporal scheduling method based on user-personalized navigation. Applied Energy 2025;378:124800. https://doi.org/10.1016/j.apenergy.2024.124800.
[6] Çelik D, Khan MA, Khosravi N, Waseem M, Ahmed H. A review of energy storage systems for facilitating large-scale EV charger integration in electric power grid. Journal of Energy Storage 2025;112:115496. https://doi.org/10.1016/j.est.2025.115496.
[7] Lappalainen K, Valkealahti S. Sizing of energy storage systems for ramp rate control of photovoltaic strings. Renewable Energy 2022;196:1366–1375. https://doi.org/10.1016/j.renene.2022.07.069.
[8] Zheng X, Bai F, Zhuang Z, Jin T. A novel hierarchical power allocation strategy considering severe wind power fluctuations for wind-storage integrated systems. International Journal of Electrical Power and Energy Systems 2023;153:109363. https://doi.org/10.1016/j.ijepes.2023.109363.
[9] Talvi M, Roinila T, Lappalainen K. Effects of ramp rate limit on sizing of energy storage systems for PV, wind and PV–wind power plants. Energies 2023;16:4313. https://doi.org/10.3390/en16114313.
[10] Arévalo P, Jurado F. Performance analysis of a PV/HKT/WT/DG hybrid autonomous grid. Electrical Engineering 2021;103:227–244. https://doi.org/10.1007/s00202-020-01065-9.
[11] Alilou M, Younesi A, Siano P. A sustainable approach to hybrid microgrid design: Optimal sizing and energy management. Renewable Energy 2026;256:124078. https://doi.org/10.1016/j.renene.2025.124078.
[12] Lappalainen K, Kleissl J. Sizing of stationary energy storage systems for electric vehicle charging plazas. Applied Energy 2023;347:121496. https://doi.org/10.1016/j.apenergy.2023.121496.
[13] Ligen Y, Vrubel H, Girault H. Local Energy Storage and Stochastic Modeling for Ultrafast Charging Stations. Energies 2019;12:1986. https://doi.org/10.3390/en12101986.
[14] Lappalainen K, Kleissl J. Effects of Capacity Factor on Sizing of Energy Storage Systems for Electric Vehicle Charging Plazas. In Proceedings of 2023 IEEE Innovative Smart Grid Technologies - Asia Conference, pp. 1–5. https://doi.org/10.1109/ISGTAsia54891.2023.10372638.
[15] Hussain A, Bui V-H, Kim H-M. Optimal Sizing of Battery Energy Storage System in a Fast EV Charging Station Considering Power Outages. IEEE Transactions on Transportation Electrification 2020;6:453–63. https://doi.org/10.1109/TTE.2020.2980744.
[16] Ali AY, Hussain A, Baek J-W, Kim H-M. Optimal operation of static energy storage in fast-charging stations considering the trade-off between resilience and peak shaving. Journal of Energy Storage 2022;53:105197. https://doi.org/10.1016/j.est.2022.105197.
[17] Hussain A, Bui V-H, Baek J-W, Kim H-M. Stationary Energy Storage System for Fast EV Charging Stations: Optimality Analysis and Results Validation. Energies 2020;13:230. https://doi.org/10.3390/en13010230.
[18] Negarestani S, Fotuhi-Firuzabad M, Rastegar M, Rajabi-Ghahnavieh A. Optimal Sizing of Storage System in a Fast Charging Station for Plug-in Hybrid Electric Vehicles. IEEE Transactions on Transportation Electrification 2016;2:443–53. https://doi.org/10.1109/TTE.2016.2559165.

[19] Jang S-R, Yoon A-Y, Kim S-S. Optimal capacity determination of photovoltaic and energy storage systems for electric vehicle charging stations. Journal of Energy Storage 2025;106:114730. https://doi.org/10.1016/j.est.2024.114730.
[20] Bryden TS, Hilton G, Dimitrov B, Ponce de León C, Cruden A. Rating a Stationary Energy Storage System Within a Fast Electric Vehicle Charging Station Considering User Waiting Times. IEEE Transactions on Transportation Electrification 2019;5:879–889. https://doi.org/10.1109//TTE.2019.2910401.
[21] Shariati O, Coker PJ, Smith ST, Potter B, Holderbaum W. An integrated techno-economic approach for design and energy management of heavy goods electric vehicle charging station with energy storage systems. Applied Energy 2024;369:123596. https://doi.org/10.1016/j.apenergy.2024.123596.
[22] Pareschi G, Küng L, Georges G, Boulouchos K. Are travel surveys a good basis for EV models? Validation of simulated charging profiles against empirical data. Applied Energy 2020;275:115318. https://doi.org/10.1016/j.apenergy.2020.115318.
[23] Majidpour M, Qiu C, Chu P, Pota HR, Gadh R. Forecasting the EV charging load based on customer profile or station measurement? Applied Energy 2016;163:134–41. http://dx.doi.org/10.1016/j.apenergy.2015.10.184.
[24] Shepero M, Munkhammar J. Spatial Markov chain model for electric vehicle charging in cities using geographical information system (GIS) data. Applied Energy 2018;231:1089–99. http://dx.doi.org/10.1016/j.apenergy.2015.10.184.
[25] Kikusato H, Fujimoto Y, Hanada S, Isogawa D, Yoshizawa S, Ohashi H, Hayashi Y. Electric Vehicle Charging Management Using Auction Mechanism for Reducing PV Curtailment in Distribution Systems. IEEE Transactions on Sustainable Energy 2020;11:1394–403. https://doi.org/10.1109/TSTE.2019.2926998.
[26] Sadeghianpourhamami N, Deleu J, Develder C. Definition and Evaluation of Model-Free Coordination of Electrical Vehicle Charging With Reinforcement Learning. IEEE Transactions on Smart Grid 2020;11:203–214. https://doi.org/10.1109/TSG.2019.2920320.
[27] Rychlik I. A new definition of the rainflow cycle counting method. International Journal of Fatigue 1987;9:119–121. https://doi.org/10.1016/0142-1123(87)90054-5.
[28] Meissner E, Richter G. The challenge to the automotive battery industry: the battery has to become an increasingly integrated component within the vehicle electric power system. Journal of Power Sources 2005;144:438–460. https://doi.org/10.1016/j.jpowsour.2004.10.031.
[29] Dallinger D, Link J, Büttner M. Fraunhofer Institute for Systems and Innovation Research. Smart grid agent: Plug-in electric vehicle, https://www.isi.fraunhofer.de/content/dam/isi/dokumente/sustainability-innovation/2013/WP08-2013_Smart-Grid-Agent-Plug-In-Electric-Vehicle.pdf; 2013 [accessed on 11.9.2025].
[30] Xu B, Oudalov A, Ulbig A, Andersson G, Kirschen DS. Modeling of Lithium-Ion Battery Degradation for Cell Life Assessment. IEEE Transactions on Smart Grid 2018;9:1131–1140. https://doi.org/10.1109/TSG.2016.2578950.

[31] Preger Y, Barkholtz HM, Fresquez A, Campbell DL, Juba BW, Romàn-Kustas J, et al. Degradation of Commercial Lithium-Ion Cells as a Function of Chemistry and Cycling Conditions. Journal of The Electrochemical Society 2020;167:120532. https://doi.org/10.1149/1945-7111/abae37.

[32] Gkavanoudis SI, Malamaki KND, Kontis EO, Shekhar A, Mushtaq U, Venu SB, Demoulias CS. Provision of Ramp-rate Limitation as Ancillary Service from Distribution to Transmission System: Definitions and Methodologies for Control and Sizing of Central Battery Energy Storage System. Journal of Modern Power Systems and Clean Energy 2023;11:1507–1518. https://doi.org/10.35833/MPCE.2022.000595.